

X-Ray Magnetic Scattering from Nonmagnetic Lu in a DyLu Alloy

B. A. Everitt, M. B. Salamon, B. J. Park, and C. P. Flynn

Department of Physics, University of Illinois at Urbana-Champaign, 1110 West Green Street, Urbana, Illinois 61801-3080

T. Thurston and Doon Gibbs

Physics Department, Brookhaven National Laboratory, Upton, New York 11973

(Received 15 May 1995)

We have detected the presence of a spin-density wave (SDW) induced in the conduction band of a $\text{Dy}_{0.60}\text{Lu}_{0.40}$ thin film alloy that orders as a c -axis helimagnet. By tuning the incident x-ray energy to the L_{III} edges, we exploit the species sensitivity of x-ray resonant magnetic scattering to isolate the contribution of each element individually. As Lu has a filled $4f$ shell, magnetic intensity observed at that resonance reflects the polarization of the $5d$ orbitals in the helical SDW. The SDW amplitude is of order $0.2\mu_B/\text{atom}$. Complementary neutron data show that the temperature dependence of the induced Lu intensity and its wave vector follow that of the total moment.

PACS numbers: 75.25.+z, 75.30.Fv, 75.50.Cc

It is generally accepted that exchange interactions in the heavy rare-earth metals (Gd to Er) are indirect, arising through the agency of spin-density oscillations induced in the $5d$ - $6s$ conduction bands by the localized $4f$ moments [1]. The conduction electron response peaks at a wave vector determined by nesting features in the Fermi surface and, in competition with the hexagonal crystal field, leads to the complex antiferromagnetic structures observed at low temperatures, including c -axis modulated, helical, cycloidal, and conical configurations [2,3]. Band structure calculations, indeed, give a good account of the periodicities observed near T_N [4]. However, direct evidence for the induced spin-density wave is sparse.

In early experimental work, Moon *et al.* [5] were able to determine the conduction electron polarization in ferromagnetic Gd by subtracting from the observed neutron scattering intensity the component attributable to the half-filled $4f$ shell of Gd. Extra intensity was observed in low-order peaks which, when combined with the excess moment measured at saturation, yielded a map of the conduction electron polarization around each Gd ion and revealed its oscillatory nature. Similar methods have been used to map the magnetic response of nonmagnetic Sc [6] and Lu [7] in a uniform field of order 6 T. In the case of Dy, which is of interest here, it is well known [8] that the saturation moment in the low-temperature ferromagnetic phase exceeds the $10\mu_B$ expected for the ${}^6H_{15/2}$ ground configuration by approximately $0.33\mu_B$. The excess is usually attributed to the conduction electron polarization, and has been detected by means of x-ray resonant scattering [9,10]. However, the induced polarization of a nonmagnetic atom has never been measured in the helimagnetic phase. In this Letter we demonstrate that it is possible to detect the conduction electron polarization induced on a nonmagnetic atom in the helical phase of a rare-earth alloy by means of the resonant scattering of x rays.

X-ray resonant magnetic scattering (XRES) [9] is an element-specific technique that exploits the anomalous cross section for x-ray scattering at an absorption edge. The XRES intensity is much larger, in general, than that of off-resonant scattering; the two processes also have different polarization characteristics. In the lanthanide series, the L_{III} edge lies in an energy range (7–10 keV) that is convenient for diffraction studies. Near the edge energy, both dipole transitions from the $2p_{3/2}$ core level to unoccupied $5d$ states and quadrupole transitions to unoccupied $4f$ levels contribute significantly to the atomic form factor for x-ray scattering. Sensitivity to magnetic order arises from the differential occupancy of spin-up and spin-down states in the vicinity of the Fermi surface. Recently, studies of the binary magnetic-rare-earth alloys $\text{Ho}_{0.5}\text{Er}_{0.5}$ [11] and $\text{Ho}_{0.5}\text{Tb}_{0.5}$ [12] using this technique have been reported. For our work, we have chosen the helimagnetic alloy $\text{Dy}_{0.6}\text{Lu}_{0.4}$, which has been found via neutron scattering [13] to order in a basal-plane spiral below 120 K. This alloy affords the opportunity to study the diffraction profiles at both the Dy (7.79 keV) and Lu (9.24 keV) L_{III} edges. Because Lu has a filled $4f$ shell, any scattered intensity that is resonant at the L_{III} edge must arise from magnetization of the $5d$ levels at the Lu site, and will therefore be a measure of the induced conduction electron polarization at the helimagnetic wave vector.

The alloy sample was grown by molecular beam epitaxy methods. Buffer layers of (110) Mo and (0001) Y were first grown on a sapphire (11 $\bar{2}$ 0) substrate, followed by deposition of $2.05\mu\text{m}$ of the $\text{Dy}_{0.6}\text{Lu}_{0.4}$ alloy. The in-plane mosaic of the sample is $\approx 0.1^\circ$, which compares well with other rare-earth epitaxial crystals; the c -axis structural coherence length is $\approx 130\text{ nm}$. Our measurements were performed at wiggler beam line X25 of the National Synchrotron Light Source. At this beam line, a cylindrically bent Si mirror and double-crystal

Si(111) monochromator collimate and filter the beam. The sample was mounted on the cold finger of a closed cycle refrigerator supported in a six-circle diffractometer. Beam size at the sample face was smaller than the $3 \times 1 \text{ mm}^2$ entrance slits. The radiation produced by the wiggler source is linearly polarized (within 1%) in the plane of the storage ring, referred to here as the σ polarization plane. We will ignore contamination by the orthogonal π component. Polarization analysis was performed by mounting a polarimeter on the detector arm. The polarimeter contains a suitable analyzer crystal and a detector positioned at a Bragg angle close to 45° . With the detector in the scattering plane, the polarimeter resolves σ -polarized scattered x rays. The analyzer crystal and detector may be rotated by 90° about the diffracted beam to detect the π -polarized scattered intensity.

The elastic scattering cross section for x-ray scattering from a single crystal is given by

$$\frac{d\sigma}{d\Omega} = r_0^2 \left| \sum_j e^{i\mathbf{Q}\cdot\mathbf{R}_j} f_j(\mathbf{Q}, \omega) \right|^2, \quad (1)$$

where r_0 is the classical radius of the electron; $\mathbf{Q} = \mathbf{k}_{\text{in}} - \mathbf{k}_{\text{out}}$, the photon momentum transfer; and $\hbar\omega$, the x-ray energy. The atomic scattering amplitude f_j consists of the usual Thomson contribution plus magnetic terms. The nonresonant magnetic amplitude may be written as

$$f_j^{\text{nonres}} = \frac{i\hbar\omega}{2mc^2} [L_j(\mathbf{Q}) \cdot \mathbf{A} + 2S_j(\mathbf{Q}) \cdot \mathbf{B}]; \quad (2)$$

the vectors \mathbf{A} and \mathbf{B} depend on the polarizations of the incoming and outgoing photons relative to their respective wave vectors. $L_j(\mathbf{Q})$ and $S_j(\mathbf{Q})$ are the Fourier components of the orbital and spin magnetization densities due to the j th atom [14]. In a helimagnet, it has been shown [15] that the signal scattered from the σ to the π channel is due to the sum of orbital and spin densities.

The resonant scattering contributions are more complex [9,16]. The electric dipole contribution at the L_{III} edge has been treated in detail by Hannon *et al.* [9] and can be approximated by

$$f_j^{E1,\text{xres}} = \frac{F_0}{E_{L_{\text{III}}} - \hbar\omega - i\Gamma/2} \times [\hat{\mathbf{e}}_{\text{out}} \cdot \hat{\mathbf{e}}_{\text{in}} n_h + i(\hat{\mathbf{e}}_{\text{out}} \times \hat{\mathbf{e}}_{\text{in}}) \cdot \hat{\mathbf{z}}_j P/4]. \quad (3)$$

Here, F_0 includes the $2p_{3/2} \rightarrow 5d$ radial matrix element, $E_{L_{\text{III}}}$ is the edge energy, and Γ is the width of the resonance. The magnetic moment of the j th ion is parallel to $\hat{\mathbf{z}}_j$. The first term, which depends on the number n_h of holes of both spins, does not reflect the magnetic order. The polarization factor can be written as

$$P = (n_{d\uparrow} - n_{d\downarrow}) - n_h \delta - \frac{n_h \Delta/2}{E_{L_{\text{III}}} - \hbar\omega - i\Gamma/2}, \quad (4)$$

where $n_{d\uparrow} - n_{d\downarrow}$ is the net number of magnetized $5d$ electrons, δ depends on the difference in radial matrix elements for spin-up and spin-down electrons, and Δ is the exchange splitting. At this level of approximation, the magnetic reflections appear only as first-order satellites of the main Bragg peaks, and only in the $\sigma \rightarrow \pi$ channel.

X-ray resonant magnetic scattering was observed at both the Dy [10] and Lu edges in the $\sigma \rightarrow \pi$ geometry, consistent with dipole selection rules. An MgO crystal was used at the Lu edge ($\theta_{\text{Bragg}}(420) = 45.4^\circ$ at 9.25 keV) and also at the Dy edge ($\theta_{\text{Bragg}}(420) = 57.7^\circ$ at 7.79 keV). The same crystal was used at both energies in order to compare directly the magnitudes of the resonant intensities. First-order helimagnetic satellites were detected about the (0002), (0004), and (0006) Bragg reflections of the alloy; they are designated as $(000\ell \pm \tau)$. At low temperatures, these were separated from the Bragg peaks by $\tau \approx 0.24$ reciprocal lattice unit (rlu), in agreement with earlier neutron scattering data from the same sample [13]. We focus mainly on the $(0002 + \tau)$ magnetic reflection, since the resonant scattering is more intense than at the $(0004 \pm \tau)$ or $(0006 \pm \tau)$ reflections and the background is lower than at the $(0002 - \tau)$ reflection. Figure 1 shows the Q -integrated intensity of the $(0002 + \tau)$ peak at 10 K as the energy was scanned through the Lu L_{III} edge (main figure) and the Dy L_{III} edge (inset), both taken with the MgO analyzer. The data are normalized to monitor counts, with the energy dependence of the monitor efficiency taken into account, and are corrected for the Lorentz factor. Polarization and

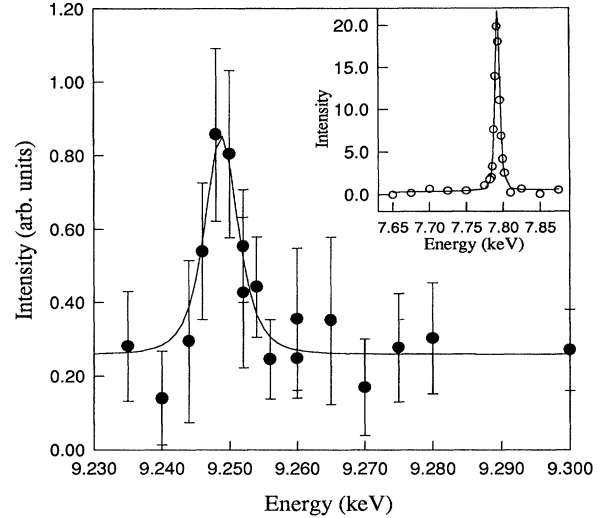


FIG. 1. Q -integrated intensity of the $(0002 + \tau)$ magnetic peak vs energy through the Lu L_{III} edge. Residual intensity is attributed to the nonresonant scattering from the Dy moments. Inset: The same, measured through the Dy L_{III} edge. An MgO (420) analyzer was used for both measurements. Lorentzian-squared curves with a FWHM of 7 eV have been fit to both data sets.

Debye-Waller corrections, which amount to $\cong 1\%$ of the intensity each, were not applied. Absorption was also not taken into account. The presence of resonant magnetic scattering at the Lu edge demonstrates the existence of an induced moment on the Lu atoms. The $\sigma \rightarrow \pi$ character of the scattering shows that it occurs within the Lu $5d$ band, and is the principal result of our paper.

Figure 2 shows the position of the $(0002 + \tau)$ magnetic peak (filled circles) as a function of temperature, with the neutron scattering data of Ref. [13] superposed. The helimagnetic wave vector is $\cong 0.265\mathbf{c}^*$ at the Néel temperature $T_N = 120$ K, and decreases with temperature before appearing to lock in to $0.240 \pm 0.001\mathbf{c}^*$ ($\cong 6/25$) below $\cong 60$ K. This may be seen more clearly in the inset to Fig. 2, where the position of the same reflection, measured at the Dy edge using a Ge(111) analyzer for better resolution, is plotted. This is a considerably tighter spiral than observed [17] in bulk Dy, where the wave vector is $0.239\mathbf{c}^*$ at T_N decreasing to $0.147\mathbf{c}^*$ at the Curie temperature $T_C = 89$ K.

The temperature dependence of the $(0002 + \tau)$ magnetic peak is shown in Fig. 3. In this figure, the Dy data were taken in the high-resolution mode (Ge analyzer) and the Lu data in the $\sigma \rightarrow \pi$ mode (MgO analyzer). Neutron scattering data are shown in the inset, for reference. Lines are drawn as a guide to the eye.

The next question we seek to address is the magnitude of the induced moment on the Lu atoms observed in Fig. 1. Each of the resonance curves shown in the figure was fit to a Lorentzian-squared profile with a FWHM of

TABLE I. Numerical values used in our calculation of the Lu induced moment. Values for the absorption coefficients were determined from analysis of the fluorescence near the edges [10].

	Dy	Lu
$\langle r \rangle$	0.00491	0.00405
Γ	7 eV	7 eV
$n_{d\uparrow} - n_{d\downarrow}$	0.357	...
δ	0.0857	$\cong 0$
Δ	0.357 eV	$\cong 0$
$\mu(7.79 \text{ keV})$	4900 cm^{-1}	1500 cm^{-1}
$\mu(9.24 \text{ keV})$	3200 cm^{-1}	4500 cm^{-1}

7 eV. Residual intensity above background at the magnetic peak position is attributed to nonresonant scattering from the Dy magnetization. We estimate the magnitude of the induced Lu moment by a direct comparison of the relative intensity of the Lu and Dy resonant signals, taking into account polarization, concentration, and absorption factors. For Lu, only the first term in the polarization factor [Eq. (4)], the net number of spin-up electrons, is nonzero. The corresponding factor P_{Dy} may be calculated by scaling the values of Δ [18] and δ [19] for Gd by the ratio of the spins; these are given in Table I. We use $n_h = 9$ for Dy [18], and average the energy-dependent denominator in Eq. (4) over the width of the resonance. An additional factor that enters into our calculation is the square of the radial matrix element $\langle r \rangle_{\text{Dy}}$ for the $2p_{3/2} \rightarrow 5d$ transition contained in F_0 of Eq. (3). Numerical values have been calculated for Dy and Lu by

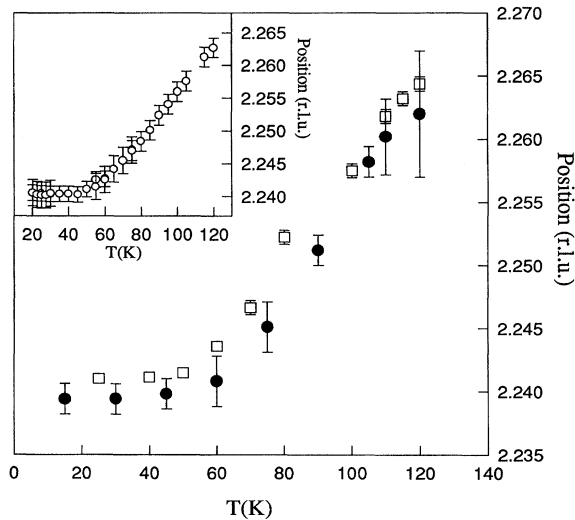


FIG. 2. Magnetic wave vector τ in units of the c -axis reciprocal lattice vector, determined from the $(0002 + \tau)$ peak. Solid circles: XRES data at the Lu edge in the $\sigma \rightarrow \pi$ configuration; squares: previous neutron scattering data. Inset: XRES data at the Dy edge, measured in the scattering plane, using a Ge analyzer for higher resolution. Below 60 K, a lock-in occurs to a value near 0.240 rlu.

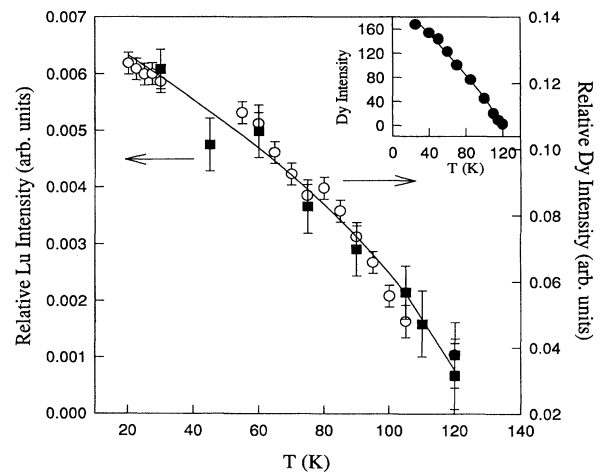


FIG. 3. Temperature dependence of the $(0002 + \tau)$ magnetic peak. Squares: Lu-edge data taken in the $\sigma \rightarrow \pi$ geometry; circles: Dy-edge data, taken in high-resolution mode. Inset: Neutron diffraction data for the same sample.

Hamrick [19]. The Lu polarization factor is then

$$|P_{\text{Lu}}| \cong \left(\frac{\langle r \rangle_{\text{Dy}}}{\langle r \rangle_{\text{Lu}}} \right)^2 \sqrt{\frac{c_{\text{Dy}} \mu(7.79 \text{ keV}) I_{\text{Lu}}}{c_{\text{Lu}} \mu(9.24 \text{ keV}) I_{\text{Dy}}} |P_{\text{Dy}}|^2}, \quad (5)$$

where the intensities I_x have been modified by the ratios of the radial matrix elements, concentrations, and absorption factors $\langle r \rangle_x$, c_x , and $\mu(E) = c_{\text{Dy}} \mu_{\text{Dy}} + c_{\text{Lu}} \mu_{\text{Lu}}$. With the values shown in Table I, we find that $P_{\text{Dy}} = -0.38$, dominated by $n_h \delta$, and that $|P_{\text{Lu}}| \approx 0.19$.

We can make a relatively simple mean-field argument that shows this to be the correct order of magnitude for the induced magnetization. While the sf interaction produces a large conduction electron polarization around each rare-earth atom, it is the net *additional s-d* polarization $\vec{\delta s}_{s-d}$ at that site, produced by neighboring rare-earth sites, that provides the indirect exchange coupling among the rare-earth magnetic moments. The resonant signal at the Dy edge measures the combination of the self-moment of that atom and the additional moment induced by its neighbors; at the Lu site, only the induced moment exists. The $s-d$ polarization produces a molecular field that acts on the rare-earth moment, which can be written as

$$\vec{H}_{\text{eff}} = \frac{(g_J - 1) j_{sf} \vec{\delta s}_{s-d}}{g_J \mu_B}, \quad (6)$$

where $j_{sf} = 0.140 \text{ eV}$ for bulk Dy [20]. In the mean-field approximation [21], we may also write \vec{H}_{eff} as

$$\vec{H}_{\text{eff}} = \lambda \vec{M} = \frac{3k_B \Theta_P}{(g_J \mu_B)^2 J(J+1)} g_J \mu_B \langle \vec{J} \rangle, \quad (7)$$

where $\Theta_P = 154 \text{ K}$ is the paramagnetic Curie temperature of bulk Dy. In the helical phase, we have $|\langle \vec{J} \rangle| = J[1 + \cos(\theta)]/2 = 0.86J$ at low temperatures where the turn angle is $\theta = 43.2^\circ$. A further reduction by the concentration of Dy atoms yields $\delta \mu_{s-d} = g \mu_B \delta s_{s-d} \approx 0.10 \mu_B$, within a factor of 2 of our experimental estimate. As was the case in extracting an experimental value, our mean field estimate is meant to be an order-of-magnitude calculation, and relies on several assumptions. Actual band calculations of the induced moment are needed both to improve on the mean field estimate of its size and to provide more reliable values of the radial matrix elements.

In summary, we have demonstrated that the element specific nature of resonant x-ray scattering permits the first observation of the helimagnetic spin density induced on the nonmagnetic constituent of a rare-earth alloy. The detection of that polarization requires the use of state-of-the-art synchrotron sources. This technique holds promise for new studies of the magnetic properties of complex materials, particularly those involving lanthanide and actinide elements. It is likely that the full potential of these methods will be realized at third-generation synchrotron sources.

We acknowledge the assistance of L. Berman at the NSLS, and helpful discussions with J. Hannon at Rice University. The neutron diffraction work was carried out at NIST in our collaboration with J. A. Borchers and R. W. Erwin. This work was supported in part by the National Science Foundation through Grant No. DMR-91-21888, and by the Department of Energy through Grant No. DEFG02-91-ER45439 (University of Illinois) and under Contract No. DE-AC02-76CH00016 (Brookhaven National Laboratory).

-
- [1] A. J. Freeman, in *Magnetic Properties of Rare-earth Metals*, edited by R. J. Elliott (Plenum Press, London, 1972), Chap. 6.
 - [2] B. R. Cooper (Ref. [1]), Chap. 2.
 - [3] J. Jensen and A. Mackintosh, *Rare Earth Magnetism*, (Clarendon Press, Oxford, 1991).
 - [4] W. E. Evenson and S. H. Liu, *Phys. Rev.* **178**, 783 (1969); S. H. Liu, R. P. Gupta, and S. K. Sinha, *Phys. Rev. B* **4**, 1100 (1971).
 - [5] R. M. Moon, W. C. Koehler, J. W. Cable, and H. R. Child, *Phys. Rev. B* **5**, 997 (1972).
 - [6] W. C. Koehler and R. M. Moon, *Phys. Rev. Lett.* **36**, 616 (1976).
 - [7] C. Stassis, B. R. Kline, C.-K. Loong, and B. N. Harmon, *Solid State Commun.* **23**, 159 (1977).
 - [8] J. J. Rhyne (Ref. [1]), p. 131.
 - [9] J. P. Hannon, G. T. Trammel, M. Blume, and Doon Gibbs, *Phys. Rev. Lett.* **61**, 1245 (1988).
 - [10] E. D. Isaacs, D. B. McWhan, D. P. Siddons, J. B. Hastings, and Doon Gibbs, *Phys. Rev. B* **40**, 9336 (1989); M. K. Sanyal, D. Gibbs, J. Bohr, and M. Wulff, *Phys. Rev. B* **49**, 1079 (1994).
 - [11] D. B. Pengra, N. B. Thoft, M. Wulff, R. Feidenhans'l, and J. Bohr, *J. Phys. Condens. Matter* **6**, 2409 (1994).
 - [12] A. Stunault, C. Vettier, F. de Bergevin, F. Maier, G. Grübel, R. M. Galéra, and S. B. Palmer, *J. Magn. Magn. Mater.* **140-144**, 753 (1995).
 - [13] B. A. Everitt, M. B. Salamon, C. P. Flynn, B. J. Park, J. A. Borchers, R. W. Erwin, and F. Tsui, *J. Appl. Phys.* **75**, 6592 (1994).
 - [14] M. Blume, *J. Appl. Phys.* **57**, 3615 (1985); M. Blume and Doon Gibbs, *Phys. Rev. B* **37**, 1779 (1988).
 - [15] Doon Gibbs *et al.*, *Phys. Rev. B* **43**, 5663 (1991).
 - [16] Jin Luo, G. T. Trammel, and J. P. Hannon, *Phys. Rev. Lett.* **71**, 287 (1993).
 - [17] W. C. Koehler (Ref. [1]), p. 81.
 - [18] B. N. Harmon and A. J. Freeman, *Phys. Rev. B* **10**, 1799 (1974).
 - [19] M. D. Hamrick, Ph. D. thesis, Rice University, 1994.
 - [20] B. Coqblin, *The Electronic Structure of Rare-Earth Metals and Alloys: the Magnetic Heavy Rare Earths* (Academic Press, New York, 1977), p. 34.
 - [21] C. Kittel, *Introduction to Solid State Physics* (John Wiley & Sons, New York, 1986), 6th ed.